

Synthesis, characterization and application of pure and modified tin (IV) Phosphate with sulfamic acid

O. E. Elmenshawy, W. S. Abo El-Yazeeda and S. A. El-Hakam

Physical Chemistry Department, Faculty of Science, Mansoura University, Mansoura, Egypt

Received: 30/12/2020
Accepted: 17/1/2021

Abstract: Tin (IV) phosphate (SnP), as a mesoporous material, was prepared through a simple one-pot synthesis method and the produced mixture was transferred into autoclave. Then, it has been modified by loading the appropriate amount of sulfamic acid (SA) using the impregnation technique. Pure and modified SnP have been characterized by using X-ray analysis (XRD) and Fourier Transform Infrared Spectroscopy (FT-IR) techniques. Acidity measurements were examined using potentiometric titration and pyridine adsorption. The total number of acid sites and Brønsted to Lewis acid sites ratio (B/L) recorded high surface acidity after loading sulfamic acid. The catalytic activity of the solid catalysts was confirmed in the synthesis of 3, 4-dihydropyrimidinone. The highest catalytic performance was displayed in the reaction in case of 25 wt% SA/SnP. Also, the adsorption behavior of Pb (II) was studied for SnP and SA/SnP. The results reported an efficient adsorbent of SA/SnP for metal.

keywords: Tin (IV) phosphate; X-ray diffraction; 3,4-Dihydropyrimidinones; Biginelli reaction

1. Introduction

The phosphates of tetravalent tin as one of non-soluble metal phosphate have many charming properties as the high thermal stability, oxidation and ion-exchange ability. It shows extremely high capacity of ion exchange ($\approx 200 \text{ mg g}^{-1}$) for cesium. Moreover, many thousands of column volumes of contaminated ground water are expected to be efficiently purified by one volume of the new layered tin (IV) phosphate [1]. Many researches have reported the good performance of gel tin phosphate material in fuel cells as a membrane inside proton exchange membrane fuel cells (PEMFC) which are widely aimed at stationary and mobile devices [2, 3]. Also, new mesoporous tin (IV) phosphate composite anode was reported. It shows superior electrochemical properties and has the highest initial capacity and excellent cycling stability [4]. Due to a very high surface area and large interlayer space of tin phosphate, it has high potential to be a good supercapacitor cathode material as well [5].

In another point of view, tin phosphate properties can be changed in the presence of various modifiers. Sulfamic acid ($\text{NH}_2\text{SO}_3\text{H}$) is one of the best available and popular effective

acids that utilized as a modifier for catalysts in organic synthesis [6, 7].

The compounds and derivatives of dihydropyrimidinone have been taken an important part in biological and pharmacological activities [8]. Anti-inflammatory, antitumor, antiviral and antibacterial actions are examples of the biological activities of these compounds [9-13]. Additionally, they exhibit various pharmacological activities such as calcium channel blockers and antihypertensive agents [14, 15]. They also act as bases in DNA and RNA. The reaction of producing these compounds was developed by Biginelli in 1891. It can be catalyzed by Lewis acids and/or Brønsted acids. The product of 3, 4-dihydropyrimidinone was synthesized in this study by multi-component chemical reaction from urea, ethyl acetoacetate and aryl aldehyde in the presence of SnP at different calcination temperatures and 25 wt% SA/SnP as catalysts.

2. Experimental

2.1. Materials

All experiments in this study require some organic and inorganic chemicals to be done in a successful way such as: stannic chloride hydrated that also called tin (IV) chloride ($\text{SnCl}_4 \cdot 5\text{H}_2\text{O}$) and phosphoric acid (H_3PO_4)

were used for the preparation of tin(IV) phosphate ($\text{Sn}_3(\text{PO}_4)_4$). Sulfamic acid (H_3NSO_3) was applied for modification of the catalyst. Urea ($\text{CO}(\text{NH}_2)_2$), benzaldehyde ($\text{C}_7\text{H}_6\text{O}$) and ethyl acetoacetate ($\text{C}_6\text{H}_{10}\text{O}_3$) were utilized for investigation of the catalytic activity. Lead nitrate, as a source of one of the heavy metals (Pb (II)), was applied for the adsorption experiments.

2.2. Preparation of the catalysts

Tin (IV) phosphate (SnP) was prepared using $\text{SnCl}_4 \cdot 5\text{H}_2\text{O}$ as a source of Sn and H_3PO_4 as phosphate source. (1.6 ml) H_3PO_4 (0.9 M) was prepared from H_3PO_4 (98%) in (30 ml) distilled water. Then colloidal solution of (7.15 gm) $\text{SnCl}_4 \cdot 5\text{H}_2\text{O}$ (98%) in water was the result of stirring. This solution was added drop-wise to H_3PO_4 (0.9 M). The resulting mixture was stirred for 2 h. at 35 °C forming white gelatin precipitate [16]. After that autoclave was used at 180 °C for 6 h. to help preparing the catalyst which denoted as SnP. And as a result SnP was washed several times with distilled water until removal of chloride ions which are tested by forming white precipitate with AgNO_3 . The precipitate of SnP was dried using rotary at 100 °C. After completely drying, the precipitate was grinded to be soft powder that has been ready to be used.

Sulfamic acid (SA) loaded on SnP was prepared by the direct impregnation method [17], in which we dissolved desired weight of SA in suitable amounts of distilled water to obtain 25 wt %. Then suspense required grams of SnP in distilled water by ultrasonication. Add this solution on dissolved SA with stirring for 2h., and then the product was left overnight, dried and calcined in a muffle furnace in air at calcination temperature of 450 °C for 4 hours to be ready for use.

2.3. Preparation of lead ions adsorbate solution

Lead ions were prepared from lead nitrate in distilled water to obtain stock solution (1000 mg/L). For each experiment, this solution should be diluted to the required concentrations.

3. Characterization techniques

3.1. X-ray analysis (XRD)

X-ray diffraction patterns of all catalysts prepared were recorded at low and high angle

by utilizing PW 150 (Philips) using Cu K α radiation source and Ni filter. The instrument was held at 40 kV and 45mA [18]. The scanning was made for a 2θ point from 0 to 70.

3.2. FT-IR analysis

FT-IR of tin phosphate catalyst and modifying one was recorded by utilizing the in situ FT-IR spectroscopic technique on a spectrometer of Nicolet magna IR 550, a resolution of 4 cm^{-1} and in 400-4000 cm^{-1} mid-IR region. Each catalyst was ground with KBr and squeezed into a fluffy wafer which was set inside the IR cell and after that the spectrum was recorded.

3.3. Surface acidity measurements

3.3.1. Non aqueous potentiometric titration

The potentiometric titration is based on the investigation of the catalysts acidity and measuring of the total number of acid sites by titration method with n-butylamine [19, 20]. This method is performed by preparation of suspension of 0.05 g of the catalyst after activation at 120 °C for 2 hrs in 10 ml acetonitrile and stirring for 2 hrs. While the titration of the suspension solution with 0.02N n-butylamine in acetonitrile at 0.1 ml/10 min, the electrode potential variation was measured by an Orion 420 digital a model using a double junction electrode. The total number of acid sites/g of catalysts was calculated using the following relation:

$$\text{Total number of acid sites/g} = \frac{\text{mL.equiv./g} \times N}{1000}$$

As N is Avogadro's number [21].

3.3.2. FTIR of pyridine adsorption

Determination of the acid sites nature for catalysts prepared and the ratio of Brønsted to Lewis acid sites was by applying the pyridine adsorption method [22]. Portions of different samples were heated for 2 hrs in vacuum oven until being at room temperature. Then, liquid pyridine was added rapidly to decrease the contact time with the atmosphere and the samples were kept to be exposed to the vapor of pyridine for one month [23]. After that, the excess of pyridine was removed by drying at 120 °C for 2 hrs and we used FT-IR spectrophotometer to perform the spectra of the samples.

3.4. Catalytic activity

3.4.1. Synthesis of 3, 4- dihydropyrimidinone

In pyrimidinones synthesis, the procedures were started by activation of the catalyst at 120° C for 2 hrs, then a mixture of (1.5 mmol) urea, (1 mmol) benzaldehyde, (1mmol) ethyl acetoacetate, (10 ml) ethanol as a solvent and the activated catalyst (0.05 g) was still stirred in round flask at 80° C for the suitable time. The reaction progress was indicated by TLC and the product was washed by ethanol and separated by simple filtration to be reused. Recrystallization of the product from ethanol and drying at 80° C [24] was occurred to get the solid product. The yield (wt %) of the product is calculated as follows [25] :

$$\text{Yield (wt\%)} = \left(\frac{\text{Obtained weight of product}}{\text{Theoretical weight of product}} \right) \times 100$$

3.5. Adsorption from aqueous solution

All measurements were applied using distilled water to prepare stock and desired solutions. We dissolved quantities of chemicals in volume of distilled water and then diluted to the required concentrations. The following equation was used to calculate the adsorbed amount at equilibrium [26]:

$$q_e = \frac{[(C_o - C_e)V]}{wt}$$

Where q_e in mg/g is the amount adsorbed at equilibrium, C_o (mg/L) is the initial concentration of solution, C_e (mg/L) is the concentration at equilibrium (mg/L), wt (g) is the adsorbent weight and V (L) is the solution volume.

3.5.1. Adsorption of lead (Pb (II)) ions

Preparation of (1000 mg/L) of a stock solution of standardized Pb (II) and the desired concentrations of experimental solutions were obtained by dilution. We investigated the effects of initial concentration, solution pH, adsorbent dose and contact time. To perform the adsorption process, the water bath shaker was used by shaking of solutions of (0.03 g) adsorbent with (50 ml) of the desired concentration of experimental solutions at controlled temperature. NaOH and HCl were added to adjust the initial pH levels. Finally, the equilibrium concentration of metal ions was determined after filtration of the supernatant

solutions by using atomic absorption spectrophotometer at various time intervals [27].

4. Results and discussion

4.1. X-Ray analysis

In Figure (1), the X-ray pattern ($2\theta = 0$ to 70°) of SnP at calcination temperatures of 350° C, 450° C and 600° C shows broad diffraction peaks that indicates amorphous structure of the sample and small crystallite size [28]. Also, the XRD pattern the samples shows an intense peak at around $2\theta = 21.08^\circ$ ($d = 4.21^\circ \text{A}$) which is observed in each one as an evidence of existence of SnP [29]. In addition, abroad band around 17.37° to 30.48° are presented in Fig. (1b) of calcined SnP at 450° C that is indicative of producing of largely amorphous material in nature [30]. Generally, the characteristic diffraction peaks of SnP have lower 2θ values that indicated an increase in the lattice constants and high surface area.

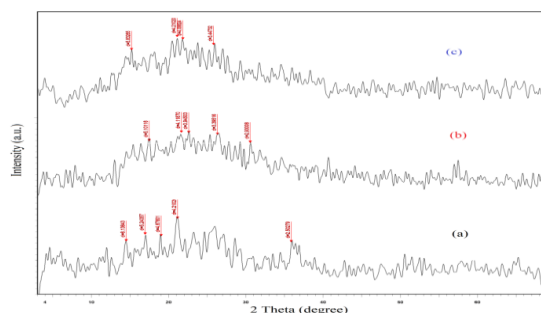


Fig (1): X-ray diffraction of calcined SnP at (a) 350° C, (b) 450° C and (c) 600° C

Figure (2) presents the XRD pattern for SnP and 25 wt% SA/SnP. We obtained broadening in the low angle diffraction region in all samples as in Fig. (2). After scanning the samples occurred from 10 to 70 degrees as presented in Fig. (2b), we found wide-range XRD patterns that display a number of peaks at 20.8° , 22.09° , 25.79° and 36.08° reflecting sulfamic acid presence [31].

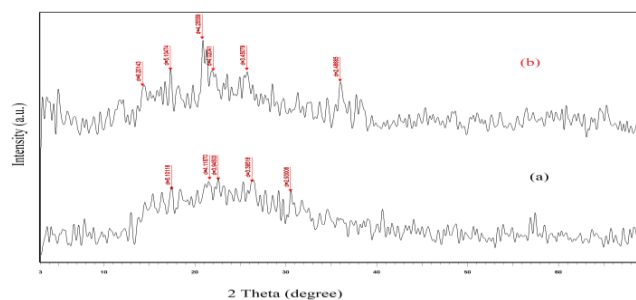


Fig (2): X-ray diffraction of (a) calcined SnP at 450° C and (b) 25 wt % SA/SnP at 450° C

4.2. FT- IR spectroscopy

Valuable information is provided about the functional groups in SnP using FT-IR analysis. Figure (3) shows the FT-IR spectra of SnP with various calcination temperatures at 350 °C, 450 °C and 600 °C. The sharp band observed in each sample at $\approx 1092\text{ cm}^{-1}$ which corresponds to the terminal PO_3 of the asymmetric stretching of Sn-O-P bond vibration, indicating the presence of phosphate [32]. The asymmetric peak of the P-O-P bridge is clearly visible in 350 °C calcined SnP at 936 cm^{-1} [33]. This peak is absent in SnP calcined at 450 °C and 600 °C suggesting the absence of P-O-P bond and proving the successful formation of Sn-O-P [34]. The band at $\approx 534\text{ cm}^{-1}$ may be attributed to the bending vibration of phosphate group [35] and the band at $\approx 616\text{ cm}^{-1}$ can be assigned to the anti-symmetric stretching mode of tin phosphate [36]. The intensity of these bands at $\approx 534\text{ cm}^{-1}$ and $\approx 616\text{ cm}^{-1}$ increases with increasing the calcination temperature of the catalyst. In addition, a sharp peak at ≈ 1629 is ascribed to H-O-H bending of water molecules with the phosphate groups. Also, the presence of a broad band between 3000 cm^{-1} and 3800 cm^{-1} may be assigned to the asymmetric stretching and vibrations of hydroxyl groups due to the interstitial water molecules [37]. But we observed the absence of the peak at $\approx 3564\text{ cm}^{-1}$ in FT-IR band of the calcined SnP at 450 °C which can be due to the loss of surface adsorbed water molecules in calcination [34].

Figure (4) shows the FT-IR analysis of SA/SnP. Its characteristics peaks are at 1402 cm^{-1} , 1630 cm^{-1} and 3421 cm^{-1} , which may be attributed to S=O, O-H and N-H, respectively.

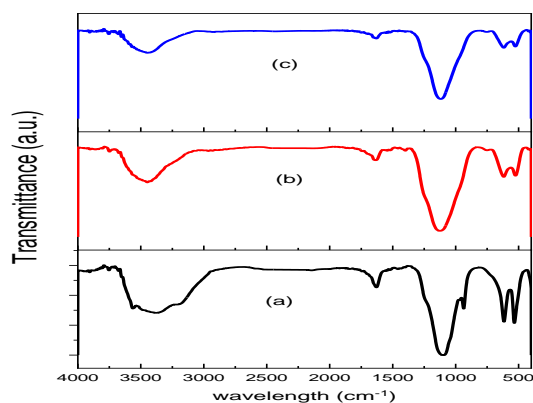


Fig (3): Fourier transform-infrared spectra of calcined SnP at 350 °C, 450 °C and 600 °C

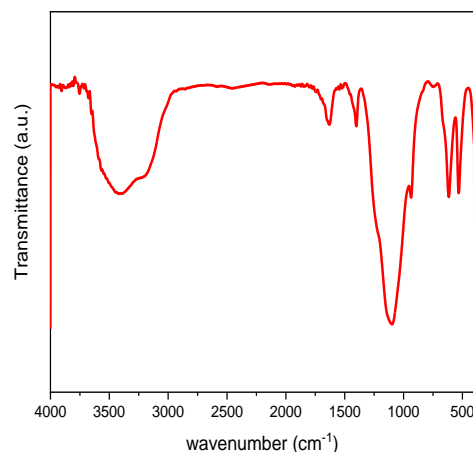


Fig (4): Fourier transform-infrared spectra of 25 wt% SA/SnP at 450 °C

4.3. Surface Acidity of the catalysts

4.3.1 Non aqueous potentiometric titration of SnP and SA/SnP

Figure (5) illustrates the electrode potential variation for SnP at different calcination temperatures. This figure indicates that the maximum acidity of calcined tin (IV) phosphate was at $E_i = 279.7\text{ mV}$, which is at 450 °C and hence, our catalyst has good acidic sites. Also, the acidity titration results of 25 wt% SnP-SA is more than that of SnP as shown in Fig. (6). The results of acidity measurements in Table (1) illustrate that calcination and the addition of sulfamic acid were followed by an increase in the acid strength and the total number of acid sites till reach the maximum at 450 °C SnP and 25 wt % SnP-SA.

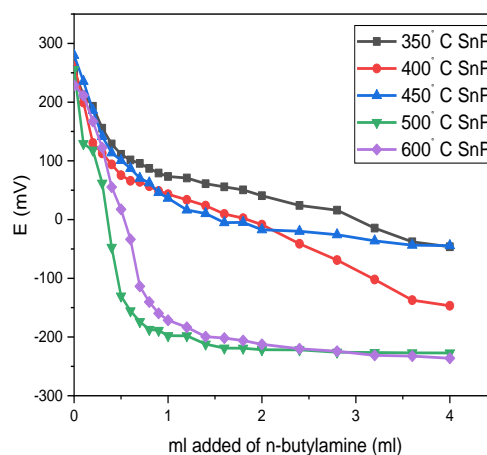


Fig (5): Potentiometric titration of n-butylamine in acetonitrile for calcined SnP at different temperatures

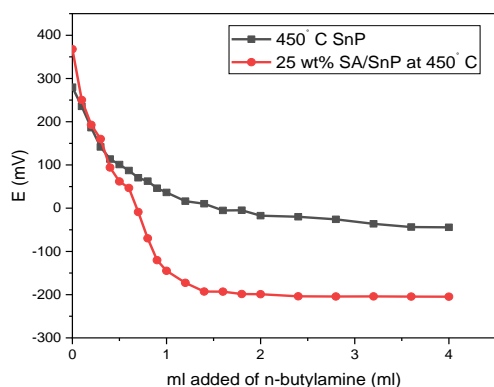


Fig (6): Potentiometric titration of n-butylamine in acetonitrile for SnP at 450 °C and 25 wt % SA/SnP at 450 °C

Table (1): Acidic properties of SnP and SA/SnP

Samples	E_i (mV)	No. of acid sites/g $\times 10^{-20}$
SnP at 350 °C	253	1.24
SnP at 400 °C	261.9	1.46
SnP at 450 °C	279.7	1.59
SnP at 500 °C	255.4	1.25
SnP at 600 °C	228.6	0.99
25wt%SA/SnP at 450 °C	367.8	2.77

4.3.2 FT-IR of pyridine adsorption of SnP and SA/SnP

FT-IR spectra of pyridine chemisorption are used to monitor the acidic properties of the samples. This is due to the lone pair of electrons on nitrogen of pyridine molecule which can coordinate with the metal atom and the acidic proton on the surface of the catalyst and then record various characteristic stretching vibrations of IR spectra in 1400-1600 cm^{-1} region. Figure (7) shows the FT-IR of pyridine adsorption of SnP catalysts with different calcination temperatures [38]. The FT-IR band at 1545 cm^{-1} could be attributed to the characteristic protonation of pyridine onto Brønsted acid sites, while the band at 1459 cm^{-1} is assigned to pyridine adsorbed on Lewis acidic sites [39]. The Brønsted acidity generates from the presence of P-OH groups, whereas Lewis acidity arises from the formation of tin in tetra-coordinated (Sn (IV)) sites within the SnP framework. The Brønsted to Lewis acidity ratio can be calculated by integrating the areas under the bands of pyridine adsorption at 1545 cm^{-1} and 1459 cm^{-1} as shown in Table (2). The pyridine-adsorbed FT-IR spectra of calcined SnP catalyst at different temperatures illustrate the decreasing in both Brønsted and Lewis

acidic sites with calcination temperature increases, but it exposes higher concentration of Lewis acid sites than Brønsted ones that indicated better catalytic activity (Fig. (7)). In addition, Figure (8) illustrates larger amount of Brønsted acid sites of SnP than that of SA/SnP, which may cause a decrease in reaction rate by SnP. Hence, increasing of Lewis acid sites and decreasing of Brønsted acid sites in the catalysts were led to catalysts with longer lifetime. The B/L ratio of SA/SnP is less than its value in SnP, in contrast to the total amount of acid sites Table (2), which resulted in high reaction rate for SA/SnP [40].

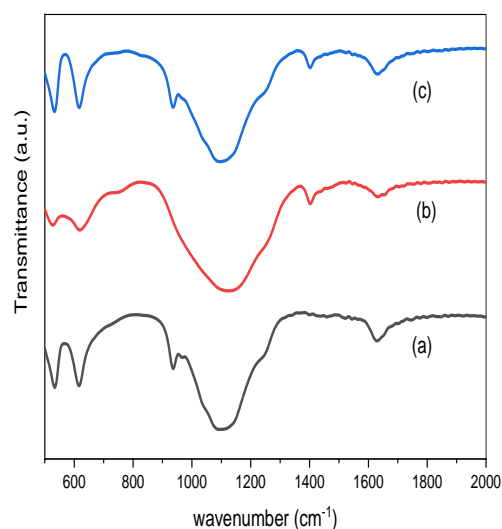


Fig (7): FTIR spectra of pyridine adsorption of (a) 350 °C, (b) 450 °C and (c) 600 °C SnP

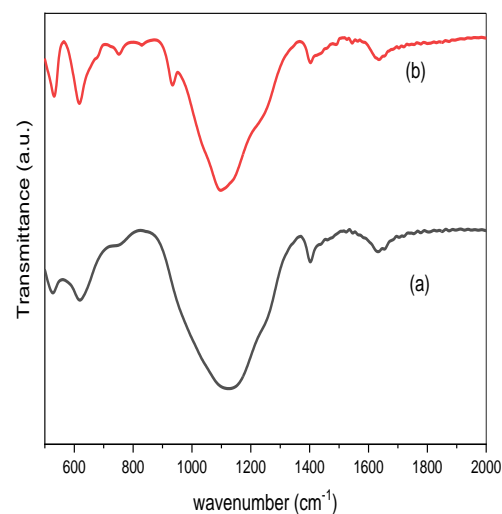


Fig (8): FTIR spectra of pyridine adsorption of (a) SnP calcined at 450 °C and (b) 25 % SA/SnP at 450 °C

Table (2): B/L ratio for calcined SnP and SA/SnP

Sample	No. of acid sites/g $\times 10^{20}$	B/L ratio
SnP at 350 °C	1.24	0.87
SnP at 450 °C	1.59	0.63
SnP at 600 °C	0.99	0.95
25 wt% SA/SnP at 450 °C	2.77	0.35

4.4. Catalytic activity

4.4.1. Synthesis of 3, 4-dihydropyrimidinones (Biginelli reaction)

The procedures were started by activation of the catalyst at 120 °C for 2 hrs, then a mixture of (1.5 mmol) urea, (1mmol) benzaldehyde, (1mmol) ethyl acetoacetate, (10 ml) ethanol as a solvent and the activated catalyst (0.05 g) was still stirred in round flask at 80 °C for the suitable time. For the sample SnP calcined at different temperatures, the yield increases from 50.61% at 350 °C to 75.21% at 450 °C then decreasing occurs at 500 °C and 600 °C as shown in Table (3) and Figure (9). The yield of 3, 4-dihydropyrimidinone increases by using 25% SA/SnP at 450 °C catalyst to reach the conversion yield of 82.7% as indicated from Fig (10) and the data presented in Table (3). Also, Table (4) and Figure (11) illustrated The relationship between the B/L ratio and calcination temperatures for the formation of 3, 4-dihydropyrimidinone for SnP.

Table (3): Catalytic activity of calcined SnP and SA/SnP catalysts for the synthesis of 3, 4-dihydropyrimidinones

Calcined catalyst	Yield of 3,4-dihydropyrimidinones (%)
SnP at 350 °C	50.61
SnP at 400 °C	58.46
SnP at 450 °C	75.21
SnP at 500 °C	51.15
SnP at 600 °C	48.31
25% SA/SnP at 450 °C	82.70

Table (4): Catalytic activity for the synthesis of 3, 4-dihydropyrimidinones and the Brønsted to Lewis acidity ratio of calcined SnP and SA/SnP catalysts

Sample	Yield of 3,4-dihydropyrimidinones (%)	B/L ratio
SnP at 350 °C	50.61	0.87
SnP at 450 °C	75.21	0.63
SnP at 600 °C	48.31	0.95
25wt% SA/SnP at 450 °C	82.70	0.35

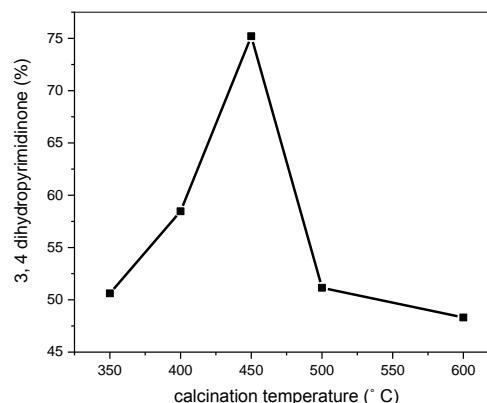


Fig (9): Effect of calcination temperatures on synthesis of 3, 4-dihydropyrimidinones.

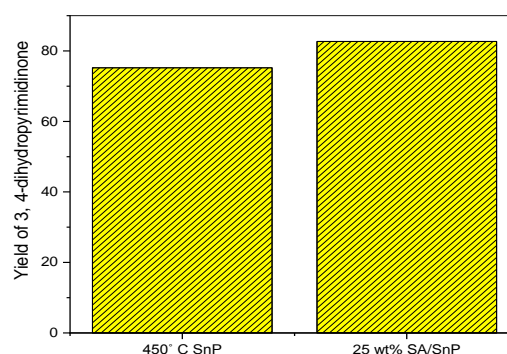


Fig (10): The yield of 3, 4-dihydropyrimidinones using SnP calcined at 450 °C and 25 wt% of SA/SnP at 450 °C

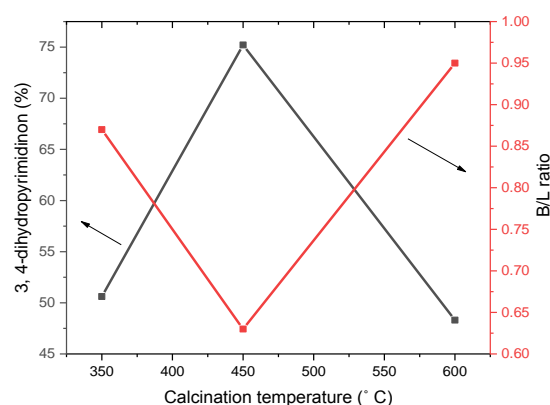


Fig (11): The relationship between the B/L ratio and calcination temperatures for the formation of 3, 4-dihydropyrimidinone for SnP

4.5. Adsorption of Pb (II) by SnP and modified SnP

We used SnP and SA/SnP to remove the harmful contaminates (Pb (II)) by adsorption which controlled physically and chemically. The adsorption process was performed for pure

calcined SnP at 450 °C and the removal of Pb (II) was 89.8 % that confirms the ability of tin (IV) phosphate to capture materials in chemisorption and physisorption processes. By loading sulfamic acid on the surface of SnP, we found increasing in the adsorption capacity of lead ions on the surface of our adsorbent (SA/SnP) to 96.24 % and this increase can be resulted from rising of active sites as shown in Figure (12).

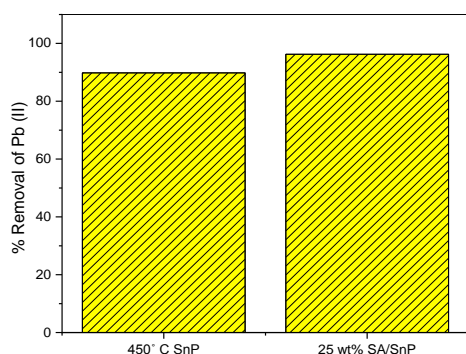


Fig (12): % Removal of Pb (II) using SnP at 450 °C and 25 wt% SA/SnP at 450 °C.

5. Conclusion

In summary, we have prepared one of the most important metal phosphates which are tin (IV) phosphates. The catalyst was modified using sulfamic acid. The catalysts were characterized by XRD and FT-IR. The modification of SnP by 25 wt% sulfamic acid at 450 °C obviously increased the surface acidity and catalytic activity in the synthesis of 3, 4-dihydropyrimidinone. The B/L ratio of SA/SnP is less than its value in SnP, which resulted in high reaction rate for SA/SnP. The adsorption process confirms the ability of tin (IV) phosphate for removal of lead. The adsorption capacity increased to 96.24% on the surface of the adsorbent of SA/SnP and this increase can be resulted from rising of active sites.

6 References

1. A. I. Bortun, S. A. Khainakov, L. N. Bortun, E. Jaimez, Jose´ R. Garcı´a, A. Clearfield, (1999) *Materials Research Bulletin*, **34**(6), 921-932.
2. G. Alberti, M. Casciola, *Annu. Rev. (2003) Mater. Res.*, **33**, 129-154.
3. C. M. Wang, E. Chalkova, C. D. Lute, M. V. Fedkin, S. Komarneni, T. C. M. Chung, S. N. Lvov, (2010) *J. Electrochem. Soc.*, **157**, B1634-B1642.
4. E. Kim, D. Son, T. Kim, J. Cho, B. Park, K. Ryu, S. Chang, (2004), *Angew. Chem.*, **116**, 6113-6116.
5. W. Huang, S. Komarneni, Y. D. Noh, J. Ma, K. Chen, D. Xue, X. Xueab, B. Jiang, (2018), *Chem. Commun.*, **54**, 2682-2685.
6. A. Rostami, A. Yari, (2012), *J. Iran. Chem. Soc.*, **9**, 489-493.
7. A. Rostami, J. Akradi, *Chin. (2011), Chem. Lett.*, **22**, 1317-1320.
8. Y. Moussaoui, R. Ben Salem, (2013), *J. Heterocycl. Chem.*, **50**, 1209-1212.
9. C.O. Kappe, *Eur. (2000) , J. Med. Chem.*, **35**, 1043-1053.
10. C. O. Kappe, *Acc. (2000), Chem. Res.*, **33**, 879-888.
11. M. B. Deshmukh, S. M. Salunkhe, D. R. Patil, P. V. Anbhule, (2009), *Eur. J. Med. Chem.*, **44**, 2651-2654.
12. B. K. Singh, M. Mishra, N. Saxena, G. P. Tripathi, *Eur. J. Med. Chem.*, (2008), **43**, 2717-2723.
13. L. Ismaili, A. Nadaradjane, L. Nicod, C. Guyon, A. Xicluna, B. Refouvelet, (2008), *Eur. J. Med. Chem.*, **43**, 1270-1275.
14. K. S. Atwal, B. N. Swanson, S. E. Unger, D. M. Floyd, S. Moreland, A. Hedberg, B. C. O. Reilly, (1991), *J. Med. Chem.*, **34**, 806-811.
15. G. C. Rovnyak, K. S. Atwal, A. Hedberg, S. D. Kimball, S. Moreland, J. Z. Gougoutas, B. C. O. Reilly, J. Schwartz, M. F. Malleys, (1992) *J. Med. Chem.*, **35**, 3254-3263.
16. Q. Hou, M. Zhen, L. Liu, Y. Chen, F. Huang, S. Zhang, W. Li, M. Ju, (2018), *Applied Catalysis B: Environmental*, **224**, 183-193.
17. S. A. El-Hakam, S. E. Samra, Sh. M. El-Dafrawy, A. A. Ibrahim, R. S. Salama, A. I. Ahmed, *RSC Adv.*, (2018), **8**, 20517.
18. H. Huang, Z. Yue, G. Li , X. Wang, J. Huang, Y. Du, P. Yang, (2013), *Journal of Materials Chemistry A*, **47**, 15110-15116.
19. K. N. Rao, K. M. Reddy, N. Lingaiah, I. Suryanarayana, P. S. S. Prasad, *J. App. Catal. A: Gen.*, (2006), **300**, 139-146.
20. A. I. Ahmed, A. S. Khdr, *App. Catal. A: Gen.*, (2009), **354**, 153-160.

21. M. N. Gatti, M. D. Mizrahi, J. M. Ramallo-Lopez, F. Pompeo, G. F. Santori, N.N. Nichio, (2017), *Applied Catalysis A: General*, **548**, 24-32.
22. H. Matsushashi, H. Motoi, K. Arata, (1994), *Catal. Lett.*, **26**, 325-328.
23. H. Doweidar, G. El-Damrawi, M. Al-Zaibani, (2013), *Vibrational Spectroscopy*, **68**, 91-95.
24. Z.-L. Zhou, P.-C. Wang, M. Lu, Chin. (2016) *Chem. Lett.*, **27**, 226-230.
25. N.G. Khaligh, F. Shirini, *Ultrasonics* (2015), *sonochemistry*, **22**, 397-403.
26. H. Parab, M. Sudersanan, N. Shenoy, T. Pathare, B. Vaze, *CLEAN–Soil, (2009) Air, Water*, **37(12)**, 963-969.
27. C. Zhu, X. Dong, Z. Chen, R. Naidu, (2016), *Int .J. Environ. Sci. Technol.*, **13**, 1257–1268.
28. D. Pathania, M. Thakur, G. Sharma, A.K. Mishra, (2018) *Materials Today Communications*, **14**, 282-293.
29. H. Yuana, N. Zhangb, L. Tian, L. Xua, Q. Shaoa, S. D. A. Zaidia, J. Xiaob, J. Chena, (2020) *Journal of Energy Chemistry*, **53**, 99-108.
30. B. M. Azmi, S. M. Hasanaly, M. Zakaria, (2012), *Advanced Materials Research*, **545**, 175-181.
31. S. A. El-Hakam, S. E. Samra, Sh. M. El-Dafrawy, A. A. Ibrahim, R. S. Salama and A. I. Ahmed, (2018), *The Royal Society of Chemistry*, **8**, 20517–20533.
32. X. Wang, F. Liang, Ch. Huang, Y. Lia, B. Chena, (2015), *Catalysis Science & Technology*, **5**, 4410-4421.
33. J. Lee, D. Son, Ch. Kim, B. Park, (2007), *Journal of Power Sources*, **172**, 908–912.
34. K. T. V. Rao, S. Souzanchi, Z. Yuan, M. B. Ray, Ch. (Charles) Xu, *RSC Adv.*, (2017), **7**, 48501-48511.
35. B. S. Rathore, D. Pathania(2014), *Journal of Alloys and Compounds*, **606**, 105–111.
36. K. Sirohi, S. Kumar, V. Singh, A. Vohra, (2018), *Acta Metallurgica Sinica(English Letters)*, **31(3)**, 254-262.
37. L. He, G. Dong, Ch. Deng, *Ceramics International*, 2016, **42**, 11918-11923.
38. K. Jagadeesw araiyah, C. Ramesh Kumar, P. S. Sai Prasad, N. Lingaiah, *Catal. .*, (2014) *Sci. Technol*, **4**, 2969–2977.
39. X. Wang, F. Liang, C. Huang, Y. Li, B. Chen, *Catal. Sci. Technol.*, (2015), **5**, 4410–4421.
40. K. Ren, D. Kong, X. Meng, X. Wang, L. Shi, N. Liu, (2019) *Journal of Saudi Chemical Society*, **23**, 198-204.